

Analyst

Accepted Manuscript



This is an *Accepted Manuscript*, which has been through the Royal Society of Chemistry peer review process and has been accepted for publication.

Accepted Manuscripts are published online shortly after acceptance, before technical editing, formatting and proof reading. Using this free service, authors can make their results available to the community, in citable form, before we publish the edited article. We will replace this *Accepted Manuscript* with the edited and formatted *Advance Article* as soon as it is available.

You can find more information about *Accepted Manuscripts* in the [Information for Authors](#).

Please note that technical editing may introduce minor changes to the text and/or graphics, which may alter content. The journal's standard [Terms & Conditions](#) and the [Ethical guidelines](#) still apply. In no event shall the Royal Society of Chemistry be held responsible for any errors or omissions in this *Accepted Manuscript* or any consequences arising from the use of any information it contains.

1
2
3
4 3D-Printed Fluidic Devices Enable Quantitative Evaluation
5 of Blood Components in Modified Storage Solutions for
6 Use in Transfusion Medicine
7
8
9

10
11
12
13
14 *Chengpeng Chen, Yimeng Wang, Sarah Y. Lockwood and Dana M. Spence*

15
16 *Department of Chemistry*

17
18 *Michigan State University*

19
20 *East Lansing, MI, 48824*

21
22 *dspence@chemistry.msu.edu*
23
24
25
26
27
28
29
30
31
32
33
34
35
36
37
38
39
40
41
42
43
44
45
46
47
48
49
50
51
52
53
54
55
56
57
58
59
60

Introduction

1
2
3
4
5
6 It is estimated that over 16 million units of stored blood are required for transfusion medicine
7
8 each year in the United States.¹ However, complications related to transfusion of blood
9
10 components still exist and a major effort to determine factors that are considered determinants
11
12 of those complications is ongoing.^{2,3} Recently, the levels of *in vivo* nitric oxide (NO) following
13
14 transfusion have been investigated and strategies to enhance concentrations of this powerful,
15
16 gaseous signaling molecule have been reported.⁴ Motivation for such studies are supported by
17
18 the fact that patients who receive a transfusion, suffer from insufficient nitric oxide bioavailability
19
20 (INOBA);⁵ as a determinant of blood flow, reductions in bioavailable NO would hinder flow of
21
22 transfused erythrocytes (ERYs), and impair their ability to deliver oxygen to demanding tissues
23
24 and organs.
25
26

27
28 There are multiple proposed sources of NO in the bloodstream, including NO release from the
29
30 ERY itself^{6,7} or production by other cell types after stimulation by ATP released from the
31
32 ERYs.^{8,9} Interestingly, McMahon has shown that the ability of the stored ERYs to release ATP
33
34 in response to hypoxic conditions is decreased during storage duration.¹⁰ In support of these
35
36 data, using an *in vitro* model of the bloodstream/endothelium interface, we recently showed that
37
38 reduced flow-induced ATP release from stored ERYs has a direct effect on endothelium-derived
39
40 NO production. The inability of the stored ERYs to release normal levels of ATP, which is highly
41
42 dependent upon the health of the cell, may not be surprising when one considers the various
43
44 chemical and physical changes of the ERYs during storage.¹¹ Collectively, these changes
45
46 (often referred to as the red cell storage lesion) are thought to have a significant effect, *in vivo*,
47
48 after transfusion has occurred.^{12,13} The exact cause of the storage lesion is not completely
49
50 understood, thus promoting various modifications to blood collection and storage solutions, as
51
52 well as overall blood component storage strategies, to help reduce the occurrence of storage
53
54 lesion.
55
56
57
58
59
60

1
2
3 The currently approved environment into which ERYs are collected and stored is quite different
4 from *in vivo* conditions. For example, the bloodstream glucose concentration of a healthy, non-
5 diabetic human is typically in the range of 5-6 mM.¹⁴ During the blood storage process, ERYs
6 are collected, and stored in solutions that have initial glucose concentrations > 110 mM.¹⁵ After
7 the addition of the ERYs to the final storage solution, the final glucose concentration is
8 approximately 40 mM, still much higher than the glucose levels in healthy individuals. While
9 there is minimal clinical evidence suggesting that the high glucose level in storage solutions is
10 the main contributor to the ERY storage lesion, there have been reports showing increased
11 advanced glycation endproducts (AGE) on ERYs as the storage duration increased.¹⁶ Also, in
12 an *in vitro* based study, our group recently reported that the collection and storage solutions
13 themselves may adversely affect the ability of the stored ERYs to release ATP, a recognized
14 stimulus of NO production in the endothelium and other cell types. Specifically, it was shown
15 that a modification of the glucose levels in the popular AS-1 storage solution from approximately
16 110 mM to 5.5 mM resulted in significantly enhanced ATP release from these cells, as well as a
17 significant increase in NO production by an immobilized endothelium. The enhancement in NO
18 production occurred even after 36 days of storage¹⁷. However, each time a measurement was
19 performed during this period, a new microfluidic device (made from
20 poly(dimethylsiloxane), PDMS) was required because the devices were not reusable. Previous
21 devices contained an irreversibly sealed membrane, which results in a device that is essentially
22 single-use. Furthermore, while the PDMS-based devices have a very high experimental
23 success rate, they typically leak between seals after multiple hours (e.g., >8) of use.
24 Furthermore, fabrication of a single device takes hours to complete due to the multiple
25 laboratory steps that must be completed to obtain a finished device. To decrease variability in
26 measurements, an ideal situation would be to employ a single device that was easy to
27 construct, yet be rugged and robust to allow multiple determinations on the stored cells over
28 periods of days to weeks.
29
30
31
32
33
34
35
36
37
38
39
40
41
42
43
44
45
46
47
48
49
50
51
52
53
54
55
56
57
58
59
60

1
2
3 Recently, three dimensional (3-D) printing has been utilized in research laboratories to construct
4 scaffolds for tissue growth¹⁸, pneumatics¹⁹, and fluidics²⁰. 3-D printing is achieved using an
5 additive process, where successive layers of materials are laid down to create a shape²¹, and
6 has been commonly used in manufacturing industries to produce design prototypes²².
7
8 Importantly, in contrast to devices prepared by soft-lithographic methods, 3-D printed devices
9 require no wet laboratory steps; the device is software designed and sent to the printer.
10
11 Therefore, depending on device complexity, obtaining a finished device can be faster than other
12 fabrication methods. Here, a fluidic device fabricated by 3-D printing technology is used to
13 evaluate ERYs stored in AS-1 (a currently approved storage solution) and AS-1N (a version of
14 AS-1 with modified glucose concentrations). Importantly, upon characterization and validation
15 of the device performance, a week-long evaluation of ERYs was performed using a single 3-D
16 printed device. Our results suggest we demonstrate that reduced glucose levels in the storage
17 solution result in a significantly increased amount of ATP released from the stored ERYs.
18
19 Further more, a single 3-D printed device was used throughout the week-long study, thus
20 reducing variability in measurements caused by use of multiple devices.
21
22
23
24
25
26
27
28
29
30
31
32
33
34
35

36 **Results and Discussion**

37 **Design and Fabrication of Device**

38
39
40 As shown in Figure 1A, the device is modeled after the dimensions of a standard 96-well plate,
41 making it suitable for direct analysis on a plate reader and use with automated fluidic handling
42 systems. The printed column (1 to 12) and row (A to H) markers make it easy to identify and
43 label wells. This particular device enables parallel analyses as it consists of six channels, each
44 with 3 wells. Membrane inserts, which are removable trans-well inserts often used in cell
45 culture applications, were plugged into the wells (Figure 1B). 3-D printed threads were designed
46 for both ends of each channel to allow for an amenable connection to external tubing via male
47
48
49
50
51
52
53
54
55
56
57
58
59
60

1
2
3 leur lock adapters (Figure 1C). The static wells between channels enable simultaneous
4 calibration and/or internal standards when necessary. In this current application, all 3 wells
5 above each channel were used for dynamic determination of ATP release from ERYs flowing
6 through the channel, while the 4 wells not over a channel were used for calibration by
7 performing static measurements of ATP standards. In this construct, quantitative determinations
8 of ATP could be performed, facilitated by a generated working curve on a single device. Figure
9 1D displays the cross section of a single channel, enabling a view of each membrane insert
10 after placement into the device. An evaluation of Figure 1D also shows how diffusion of the
11 analytes could occur, moving from the channel, across the membrane, and to the area above
12 the insert for eventual measurement. In this study, ATP diffuses from channels to wells, where it
13 is collected into buffer already loaded into the well insert prior to commencement of pumping.
14 Based on diffusion, the amount of ATP accumulated in the well (at some fixed pumping time) is
15 proportional to the concentration in the channel, thereby enabling ATP that is in the channel to
16 be quantitatively determined. After flow of samples in the channels, the device was detached
17 from tubing and directly placed into the plate reader for measurements (Figure 1E). A more
18 detailed schematic of the entire device design can be seen in Figure S1 in Supplementary
19 Information. Device and well alignment in the plate reader were characterized and validated
20 prior to studies involving ATP by using fluorescein standards ranging from 0 to 20 μM in the
21 membrane inserts, followed by linear regression analysis of the standards as shown Figure S2
22 in Supplementary Information.

23 24 25 26 27 28 29 30 31 32 33 34 35 36 37 38 39 40 41 42 43 44 45 46 47 48 **Evaluation of Device Ruggedness**

49
50 The trans-well inserts are not fixed into place by any type of glue or epoxy adhesives that lead
51 to permanent combination. There is, however, a wrap of PTFE tape around the side of inserts to
52 help them seal onto the bulk device tightly, yet remain removable if needed. However, to
53 confirm that bulk fluid movement is not occurring from the channel to the area above the
54
55
56
57
58
59
60

1
2
3 membrane insert, or vice-versa, 50 μL of doubly deionized water (DDW) was added into
4
5 membrane inserts in wells B1, E1 and G1 above channel 1. After circulating DDW through the
6
7 channel for 2 hours at a rate of 50 $\mu\text{L}/\text{min}$, the remaining volumes of water in the inserts were
8
9 measured. A control set was performed by adding 50 μL of DDW in inserts placed in static wells
10
11 A2, D2 and F2, and then measuring the remaining volumes after two hours loading. As shown in
12
13 Table 1, though a minimal loss of liquid volume in the dynamic inserts (B1, E1 and G1, with
14
15 flowing underneath) was observed, the lost volume was not likely due to liquid transfer into the
16
17 channel for a minimal liquid loss was also shown in static inserts (A2, D2 and F2), beneath
18
19 which, there is no channel. There is no significant difference in remaining volumes between
20
21 dynamic and static inserts. The results suggest that loaded liquid can be firmly held in dynamic
22
23 inserts without being drawn into the underlying flow channel for the time duration investigated.
24
25 The other five channels were examined in the same way, and no bulk liquid transfer was
26
27 observed. However, it should be noted that changes in flow rate, pore diameter of the
28
29 membrane, or any flow restrictors at the end of the channels will alter the direction of fluid flow,
30
31 thus resulting in either bulk fluid movement from channel to insert well or an apparent aspiration
32
33 of fluid from insert to channel.
34
35
36
37
38

39 The leakage of fluids from the flowing channel across the membrane and into any pre-loaded
40
41 reagents on the other side of the membrane have the potential to be detrimental to the quality of
42
43 analysis using this fluidic device (e.g., dilution can hinder detection limits). To determine if
44
45 flowing fluids leak across membrane (as opposed to movement of an analyte by diffusion
46
47 alone), a fluorescein solution was circulated through channel 1, with nothing loaded in the
48
49 membrane inserts above the channel. After 2 hours of pumping this solution, fluorescence
50
51 images above the channel were obtained. Figure 2 was integrated by images observed on
52
53 separate parts of the channel because of the limited camera view. As shown in Figure 2, there
54
55 is some fluorescein at the bottom of each well. This fluorescence was on the apical side of the
56
57
58
59
60

1
2
3 membrane (the bottom side, touching the channel). Due to the lack of fluorescein entering the
4 well (we would expect a “circle” of fluorescence emission in the well if flowing fluid had moved
5 across the membrane), we concluded that leakage of fluids was not occurring. The other five
6 channels were verified with the same method and none showed any leakage of liquid across
7 membrane. This is important because it will help ensure that only molecules can diffuse or move
8 through the membrane to the other side of inserts.
9
10
11
12
13
14
15
16

17 **Optimizing Device Parameters for the Quantitative Determination of ATP**

18
19
20 There are multiple factors that can affect the overall quantitative determination of ATP release
21 from the stored ERYs flowing through the device channels. One of the first factors to be
22 investigated was the amount of time the ERYs were allowed to flow through the device channel
23 prior to determination of ATP. As the ERYs pass through the channel, they release ATP that
24 diffuses through the porous membrane on the bottom of the trans-well insert. Thus, an increase
25 in the amount of time the ERYs pass through the device channels would increase the collection
26 time and amount of ATP in the well above the channel. To determine the optimal ATP collection
27 time, ATP standards (0 to 800 nM) were circulated for 10 min, 20 min or 30 min through a
28 device channel having a well insert that was loaded with 50 μ L of PSS. This circulation time
29 enabled ATP from the ERYs to diffuse through the membrane pores. After the various
30 circulation times of the ERYs (or, the collection time of ERY-derived ATP), an aliquot of a
31 luciferin/luciferase mixture was added to the well insert and the resultant chemiluminescence
32 was recorded using the multi-well plate reader. Calibration curves were prepared to investigate
33 such figures of merit as analytical sensitivity and limits of detection for each collection time. The
34 resultant data, which are summarized in Table 2 and shown graphically in Figure S3
35 (Supplementary Information), show that lower limits of detection and higher sensitivity can be
36 achieved as the collection time increased. Although quantifiable results were obtained even
37 after 10 minutes of pumping, the 20 minute collection period was utilized for subsequent studies
38
39
40
41
42
43
44
45
46
47
48
49
50
51
52
53
54
55
56
57
58
59
60

1
2
3 because of its precision and significant reduction in the limit of detection in comparison to the 10
4
5 minute pumping period and its suitability for measurements of ERY-derived ATP, which is
6
7 typically in a range of 90 to 400 nM, depending on the health status of the donor.
8
9

10
11 A mixture consisting of luciferin/luciferase is required in the chemiluminescent determination of
12
13 ATP. However, this mixture also contributes to higher background luminescence during the
14
15 measurement portion of the analysis.²³ Thus, a study was performed to determine which
16
17 volume of luciferin/luciferase mixture added during the assay provided the best analytical
18
19 features (detection limit, sensitivity, etc.). To perform this study, ATP standards of identical
20
21 concentration were circulated in a channel for 20 min and ATP was allowed to diffuse through
22
23 the membranes of the trans-well inserts that had already been filled with 50 μL of buffer, after
24
25 which, the device was detached and placed on the sample holder of the plate reader. Aliquots of
26
27 10, 20 or 30 μL of the luciferin/luciferase mixture were added to the wells and the
28
29 chemiluminescence from each trial was acquired. The data from these studies, shown in Table
30
31 3 and graphically in Figure S4 (Supplementary Information), suggest that 10 μL of the
32
33 luciferin/luciferase mixture yielded the lowest background (y-intercept), and the best linearity, as
34
35 measured by the coefficient of determination, r^2 . In fact, larger volumes of the luciferin/luciferase
36
37 mixture added to the wells lowered analysis quality, likely due to higher background emission. It
38
39 was also observed that when adding the 20 or 30 μL volumes of the luciferin/luciferase mixture,
40
41 the signals from 100 nM or 200 nM ATP standards were not statistically different and exhibited
42
43 reduced linearity and higher detection limits. A calibration curve with 20 min ATP collection time
44
45 and 10 μL of luciferin/luciferase, the optimal conditions among variations studied here, is shown
46
47
48
49 in Figure S5 in the Supplementary Information.
50
51

52 53 **Evaluation of Analytical Features of the Device** 54 55 56 57 58 59 60

1
2
3 High-throughput Evaluation. With six channels integrated into the 3-D printed device, all of
4 which were amenable to a commercial plate reader, high-throughput applications were
5 explored. Six ATP standards (0 to 0.8 μM) were circulated in the six channels, but in a random
6 order. The membrane inserts in wells B on each channel were loaded with 50 μL of PSS to
7 collect ATP by diffusion. The chemiluminescence intensity detected from each insert as a
8 function of the concentration of ATP flowing in the channels is shown in Figure S6 in the
9 Supplementary Information. The linearity ($r^2=0.99$) and precision of measurement (indicated by
10 error bars representing standard deviation) demonstrated the device can perform 6 quantitative
11 analyses, simultaneously.

12
13
14 Detection Accuracy, Intra-channel Reproducibility and Reusability Evaluation. Under optimal
15 conditions, ATP standards of known concentrations (150 nM and 250 nM) were evaluated with
16 the device. These two concentrations were determined because a 7% solution of ERYs release
17 ~ 200 nM ATP. Such measurements were performed on channels 1, 3 and 5. Data shown in
18 Table 4 indicates that the levels of ATP can be detected quantitatively, and the detection results
19 from the three channels did not show any statistically significant difference, which further
20 suggests that quantitation on different channels will yield statistically similar results. Such results
21 are expected due to all channels being printed on the same printer using the same prototype
22 dimensions. To confirm precision between channels, ATP standards were circulated in three
23 channels and resultant calibration curves were compared. As shown in Table 5, these channels
24 were statistically equal in terms of background, sensitivity, linearity, detection limit and accuracy.
25 This intra-channel reproducibility is another outstanding advantage of the 3-D printed device, as
26 it helps reduce variability of devices from different manufactures and fabrication protocols.
27 Another key advantage is the reusability of the 3-D printed device; the same device was used
28 for all reported experiments and was cleaned with a simple rinse with DDW. Data in Figure S5
29 and Figure S6 in the Supplementary Information were obtained using the same channel on the
30
31
32
33
34
35
36
37
38
39
40
41
42
43
44
45
46
47
48
49
50
51
52
53
54
55
56
57
58
59
60

1
2
3 same device. The error bars, which represent standard deviation, support the reusability of the
4 device, which not only reduces use of materials, but also enables repeated measurements of
5 the same sample on the same device in a reproducible manner.
6
7
8
9

10 **Application of the Device to Quantify ATP Released from Stored ERYs**

11
12
13 The device was next applied to quantify ATP released from ERYs stored in AS-1, and FDA-
14 approved solution and our modified solution (AS-1N). ATP release from stored ERYs has
15 recently been shown to be reduced during the storage period.¹⁷ ATP plays a key role in blood
16 flow as a recognized stimulus of NO production from endothelial cells,²⁴ which regulates vessel
17 dilation. A storage period of one week was examined and the ATP release on day 1, 3, 5, 7
18 was quantified. The data in Figure 3 provide evidence that ERYs stored in high glucose (AS-1)
19 released significantly less ATP than those stored in normoglycemic AS-1N. In fact, on day 1, or
20 after just several hours storage, a significant difference of ATP released from ERYs in the two
21 solutions was observed (in AS-1, 175.6 ± 15.5 nM ATP was released; in AS-1N, 232.3 ± 6.7 nM
22 ATP was released; $p < 0.03$). On day 3, 5 and 7, significantly less ATP was released in AS-1
23 than AS-1N ($p < 0.03$). These results further suggest that the currently approved storage
24 solution (AS-1) may have adverse effects on stored ERYs due to its hyperglycemic character,
25
26
27
28
29
30
31
32
33
34
35
36
37
38
39

40 The data in Figure 3 was acquired in two steps, measuring five ATP standards in five channels
41 first, then flowing ERY samples in two random channels for determination of released ATP. In
42 terms of analytical impact, to further examine if the device can perform calibration and sample
43 measurements in only one step, four ATP standards and ERY samples stored in AS-1 and AS-
44 1N were flowed simultaneously on the device. Panel A in Figure S7 in the Supplementary
45 Information shows the setup of such a measurement on the 3-D printed device, while panel B
46 shows an example of an acquired calibration curve. Panel C contains the quantified ATP
47 release from AS-1 and AS-1N stored ERYs over a seven day storage period. The ATP release
48
49
50
51
52
53
54
55
56
57
58
59
60

1
2
3 data is consistent with that in Figure 3, thus confirming that the device has the capability to
4 perform simultaneous calibration and sample quantification in a high-throughput manner.
5
6

7 8 **Experimental**

9 10 **Design and Fabrication of Device**

11
12 The fluidic device was printed on an Objet Connex 350 printer capable of an XY resolution of
13 600 DPI and Z resolution of 16 μm , (Stratasys Ltd, Eden Prairie, MN) in the department of
14 Electrical and Computer Engineering at Michigan State University. The 3-D design, (Figure S1
15 in Supplementary Information) was created using the CAD based engineering software²⁵
16 package AutoDesk Inventor Professional (Autodesk, Inc., San Francisco, CA). The device was
17 printed using Objet VeroClear material (Stratasys Ltd, Eden Prairie, MN) whose exact
18 composition is proprietary, but approximately contains isobornyl acrylate (15-30%), acrylic
19 monomer (15-30%), urethane acrylate (10-30%), acrylic monomer (5-10; 10-15%), epoxy
20 acrylate (5-10; 10-15%), acrylate oligomer (5-10; 10-15%), and a photoinitiator (0.1-1;1-2%).
21
22 Once printed, the device is translucent and rigid, but becomes optically transparent and ready to
23 use after a simple polish and clean with sand paper and water. Commercially available
24 membrane inserts (6.5 mm diameter; Corning, Inc., Horseheads, NY) with polyester membranes
25 (0.4 μm pore diameter) were inserted into the dynamic wells above the channels. The inserts
26 function as a semi-permeable barrier between flowing cells or reagents in the channel and
27 reagents that were loaded in the insert (on the opposite side of the membrane). This
28 configuration enables molecular transport through the pores by diffusion. The side of each
29 membrane insert was wrapped by a layer of PTFE seal tape (PL Sourcing, Inc., Newport News,
30 VA) to enhance the seal between the inserts and the wells.
31
32

33
34 A section of grafted tubing was prepared by connecting two, 20 cm pieces of 1/8" tygon tubing
35 (Saint-Gobain PPL Corp, Jackson, MI) to the ends of a piece of 15 cm Ismatec tubing (Cole-
36
37
38
39
40
41
42
43
44
45
46
47
48
49
50
51
52
53
54
55
56
57
58
59
60

1
2
3 Parmer Instrument Company, Vernou Hills, IL). The two ends of the tubing were connected to
4 male leur lock adapters (IDEX Health & Science LLC, Oak Harbor, WA), which can be
5 integrated with the two threaded ends of a channel in the printed device, thus forming a loop.
6
7 The threads were printed directly from the device design (as opposed to being tapped post-
8 printing) as 10-32 type threads, thus enabling the use of the aforementioned male leur lock
9 adaptors. Fluids or samples were driven through the loop by a 12-roller peristaltic pump (IDEX
10 Health & Science LLC, Oak Harbor, WA).
11
12
13
14
15
16
17
18

19 **Evaluation of Device Ruggedness**

20
21 To confirm the absence of bulk fluid movement through the membrane pores into a channel, a
22 50 μL aliquot of DDW was added to dynamic inserts in wells B1, E1 and G1, while DDW was
23 delivered through the closed loop system at a flow rate of 50 $\mu\text{L}/\text{min}$ for 2 hours. The amount of
24 water in each insert after pumping was determined by mass measurement. As a control group,
25 the same amount of DDW was loaded into each insert in static wells A2, D2 and F2 (no channel
26 beneath and thus no possible water delivery) for 2 hours. There is no channel underneath the
27 static inserts, thus representing a control group used to account for any change in volumes in
28 the inserts due to evaporation. All other channels were examined in the same way, using static
29 inserts in the next right column as a control set.
30
31
32
33
34
35
36
37
38
39
40
41
42

43 To investigate the extent of any leakage of fluids from a channel to the area above membrane
44 inserts, a 30 μM fluorescein solution in DDW was circulated at a rate of 50 $\mu\text{L}/\text{min}$ in the loop for
45 2 hours. The device was then detached from the pumping system and placed under the
46 objective lens of a fluorescence microscope (Olympus, Japan). Leakage was investigated for all
47 six channels on the device; any detectable quantity of fluorescein on the outside of the trans-
48 well inserts was considered to be indicative of leaking.
49
50
51
52
53
54
55

56 **Optimizing Device Parameters for the Quantitative Determination of ATP**

57
58
59
60

1
2
3 ATP Collection Time Optimization. The well-established luciferin/luciferase chemiluminescence
4 assay was used for ATP assays.²⁶ Reagents were prepared by dissolving 2.0 mg of D-luciferin
5 (Sigma Aldrich, St. Louis, MO) in 5 mL of DDW, and adding the resultant solution into a single
6
7 100 mg vial of firefly extract (Sigma Aldrich, St. Louis, MO). Five ATP (Sigma Aldrich)
8 standards ranging in concentration from 0 nM to 800 nM were prepared by dissolved in DDW
9 and diluting in a physiological salt solution (PSS, contains 4.7 mM KCl, 2.0 mM CaCl₂, 1.2 mM
10 MgSO₄, 140.5 mM NaCl, 21.0 mM tris-hydroxymethyl aminomethane, 5.5 mM glucose, and 5%
11 bovine serum albumin at pH = 7.4; all reagents were from Sigma Aldrich). A 50 μL aliquot of
12 PSS was loaded in the insert located in well B. The PSS served as a solution to collect ATP
13 diffusing from the channel through the membrane of the insert. After 10 min, 20 min or 30 min of
14 pumping the various ATP standards, the device was detached and placed in the sample holder
15 of the plate reader (Molecular Devices LLC, Sunnyvale, CA). A 50 μL aliquot of 20 nM ATP
16 standard solution was pipetted into insert in static well 2A as a calibrator, thereby minimizing
17 possible indeterminate error. A 10 μL of luciferin/luciferase was then added into inserts in wells
18 2A and 1B, simultaneously. After 15 s, the chemiluminescence intensity from both inserts was
19 detected simultaneously, followed by the evaluation of the detection background, detection limit,
20 sensitivity and linearity for the different pumping times under investigation.
21
22
23
24
25
26
27
28
29
30
31
32
33
34
35
36
37
38
39
40

41 Luciferin/luciferase Assay Amount Optimization. To determine the optimal volume of
42 luciferin/luciferase mixture for each assay, ATP standards were prepared and circulated in a
43 channel, as described above, with 50 μL of PSS loaded in the insert in well 1B. ATP standards
44 circulated for 20 min at a rate 50 μL/min. Next, 10 μL to 30 μL aliquots of the luciferin/luciferase
45 mixture were added to the membrane inserts in dynamic well 1B, as well as static well 2A
46 (containing 50 μL of 20 nM ATP standard as a calibrator) simultaneously. The device was
47 detached and placed in the plate reader sample holder and the optimal assay amount was
48 determined by an evaluation of detection limit, linearity and sensitivity.
49
50
51
52
53
54
55
56
57
58
59
60

Evaluation of Analytical Features of the Device

High-throughput Evaluation. ATP solutions of 0, 0.2, 0.3, 0.4, 0.5, 0.8 μM were prepared in PSS and circulated randomly through 6 channels, simultaneously, at a rate 50 $\mu\text{L}/\text{min}$ for 20 min after 50 μL of PSS were loaded in the membrane inserts in wells B above each channel. The device was then detached from tubing and placed in the plate reader for chemiluminescence detection with the optimal ATP quantitation parameters determined above, on all wells in the row labeled as "B". A curve of chemiluminescence intensity versus ATP concentration was obtained, and the resulting regression statistics (slope, y-intercept, and coefficient of determination) were calculated.

Detection Accuracy Evaluation. ATP standards of 150 nM and 250 nM were prepared and circulated in channel 1 at a rate 50 $\mu\text{L}/\text{min}$ for 20 min, with 50 μL of PSS buffer loaded in the membrane insert in well B (dynamic wells) above the channel to collect ATP by diffusion. A 50 μL aliquot of 20 nM ATP was then added into the membrane insert in wells found in row labeled as "A" (static wells). The device was then detached from tubing and placed in the sample holder of the plate reader. Chemiluminescence was detected 15 s after adding 10 μL of the luciferin/luciferase assay into dynamic and static wells to quantify the ATP, using calibration curves prepared in advance in a similar manner as described above. Two more identical measurements were performed on channel 3 and channel 5.

Evaluation of Intra-channel Reproducibility and Reusability

ATP standards having concentrations ranging from 0 to 800 nM were prepared and simultaneously circulated through channels 1, 3 and 5 at a rate 50 $\mu\text{L}/\text{min}$ for 20 min, while 50 μL of PSS buffer were loaded in the membrane inserts in well B above each channel. After adding 50 μL of 20 nM ATP to wells 2A, 4A and 6A (as static calibrators for measurements on

1
2
3 channels 1, 3, and 5, respectively), the device was detached and placed in the sample holder of
4
5 the plate reader. An aliquot of 10 μ L of the luciferin/luciferase mixture was simultaneously
6
7 added into inserts above the dynamic and static wells, and chemiluminescence was detected by
8
9 the plate reader after 15 s. A comparison of sensitivity, detection limit and linearity of results
10
11 from the 3 channels was performed to determine if the device channels and inserts are
12
13 statistically equivalent. Precision was also investigated by performing identical measurements
14
15 as those described above while changing well inserts in between studies.
16
17
18

19 **Application of the Device to Quantify ATP Released from Stored ERYs**

20
21
22 Collection and Storage of ERYs. Citrate phosphate dextrose solution (CPD) and additive
23
24 solution 1 (AS-1) were prepared according to standard compositions found in the literature²⁷.
25
26 Specifically, 50 mL of CPD were prepared containing 89.4 mM sodium citrate, 15.6 mM citric
27
28 acid, 128.8 mM dextrose, and 16.1 mM monobasic sodium phosphate. For AS-1, 200 mL were
29
30 typically prepared containing 154.0 mM sodium chloride, 41.2 mM mannitol, 1.8 mM adenine,
31
32 and 111.1 mM dextrose (all chemicals were from Sigma Aldrich). All reagents were prepared
33
34 from solid forms and used as received without further purification. Normoglycemic versions of
35
36 CPD and AS-1 (CPD-N and AS-1N, respectively) were prepared in a manner identical to CPD
37
38 and AS-1, but with the glucose level at 5.5 mM.
39
40
41
42

43 All blood was collected by venipuncture under IRB approved protocol. The collection process
44
45 consisted of preparing 6 non-siliconized and untreated (i.e., no heparin or other anticoagulant)
46
47 10-mL glass Vacutainer tubes; 3 of these tubes contained 1 mL of CPD, while the other 3
48
49 contained 1 ml of CPD-N. Next, approximately 7 mL of whole blood were collected into each
50
51 tube, resulting in a total blood volume of \sim 8 mL. The blood remained in the collection solutions
52
53 for at least 30 min, but not more than 2 h at room temperature (\sim 20°C), prior to processing.
54
55 Whole blood processing consisted of centrifugation at 2,000g for 10 mins followed by removal of
56
57
58
59
60

1
2
3 the plasma and buffy coat layers by aspiration. Importantly, an additional top 2-mm layer of the
4 packed ERYs were also removed to minimize white cells remained during subsequent storage
5 in the AS-1 or AS-1N solutions. The purified ERYs from the 3 tubes containing CPD were then
6 combined into a 15 mL tube, followed by the addition of AS-1 such that the ratio of packed ERY
7 volume to AS-1 volume was 2:1. The same protocol was followed for ERYs collected in CPD-N
8 and stored in AS-1N. Finally, 2 mL of the ERYs (stored in the AS-1 or AS-1N) were added to
9 PVC bags at 4 °C for up to 7 days. Prior to use, the PVC bags were sterilized under UV light
10 overnight. The PVC bags were prepared in-house using rolled PVC and a heat sealer. All
11 solutions used in collection and storage were autoclaved at 10 bar and 121°C prior to use. All
12 blood collection and storage processes were performed under sterile conditions. All blood
13 collection procedures from informed and consented donors were approved by the Biomedical
14 and Health Institutional Review Board at Michigan State University.

15
16
17
18
19
20
21
22
23
24
25
26
27
28
29
30 Measurement of ATP Released from ERYs Stored in AS-1 and AS-1N. A calibration curve was
31 first prepared by flowing ATP standards (0, 0.1, 0.2, 0.4, 0.8 μM) in five channels
32 simultaneously, with 50 μL of AS-1 loaded in wells B above each channel for 20 min to collect
33 diffused ATP, which was then determined by chemiluminescence as described above. After
34 rinsing the device by DDW and AS-1, ERYs stored in AS-1 and AS-1N were diluted with
35 corresponding solution to a final hematocrit of 7%, and circulated on the device in 2 random
36 channels for 20 min at a rate 50 $\mu\text{L}/\text{min}$. An aliquot of 50 μL of the appropriate additive solution
37 was loaded in the inserts in wells B above corresponding channels to collect ATP by diffusion,
38 after which, the device was detached and placed in the plate reader, 10 μL of the
39 luciferin/luciferase assay mixture were simultaneously added into the well inserts and
40 chemiluminescence intensity was measured after 15 s. In addition, a 50 μL aliquot of 20 nM
41 ATP was added into the insert in well 2A (static well) as a calibrator during both calibration
42 curve preparation and sample measurement. To confirm that the increase in released ATP was
43
44
45
46
47
48
49
50
51
52
53
54
55
56
57
58
59
60

1
2
3 not due to cell lysis, an absorbance measurement was performed (to evaluate if free
4 hemoglobin was detected in the supernatant) after flow was concluded. If hemoglobin was
5 detected, that particular sample was discarded due to indication of lysis. In the studies reported
6 here, there were no samples discarded due to lysis.
7
8
9
10

11
12 The ATP released from ERYs was also quantified on the device in a one-step manner. Four
13 ATP standards of 0, 0.1, 0.2 and 0.4 μM in AS-1N were prepared and circulated through
14 channels 1, 3, 5 and 7, while diluted ERY samples stored in AS-1N and AS-1 were flowing in
15 channels 9 and 11. An aliquot of 50 μL of AS-1N was loaded in the inserts in wells B (dynamic
16 well) above all channels to collect ATP by diffusion for 20 min, after which the same procedures
17 as described above were taken to detect chemiluminescence intensity from wells B by the plate
18 reader. Signals from wells 1B, 3B, 5B and 7B, which corresponded to 0, 0.1, 0.2 and 0.4 μM
19 ATP flowing beneath them, respectively, were used for calibration curve, while signals from
20 wells 9B and 11B reflecting the released ATP amount from corresponding ERYs samples.
21
22
23
24
25
26
27
28
29
30
31
32

33 **Statistical Analysis of Data**

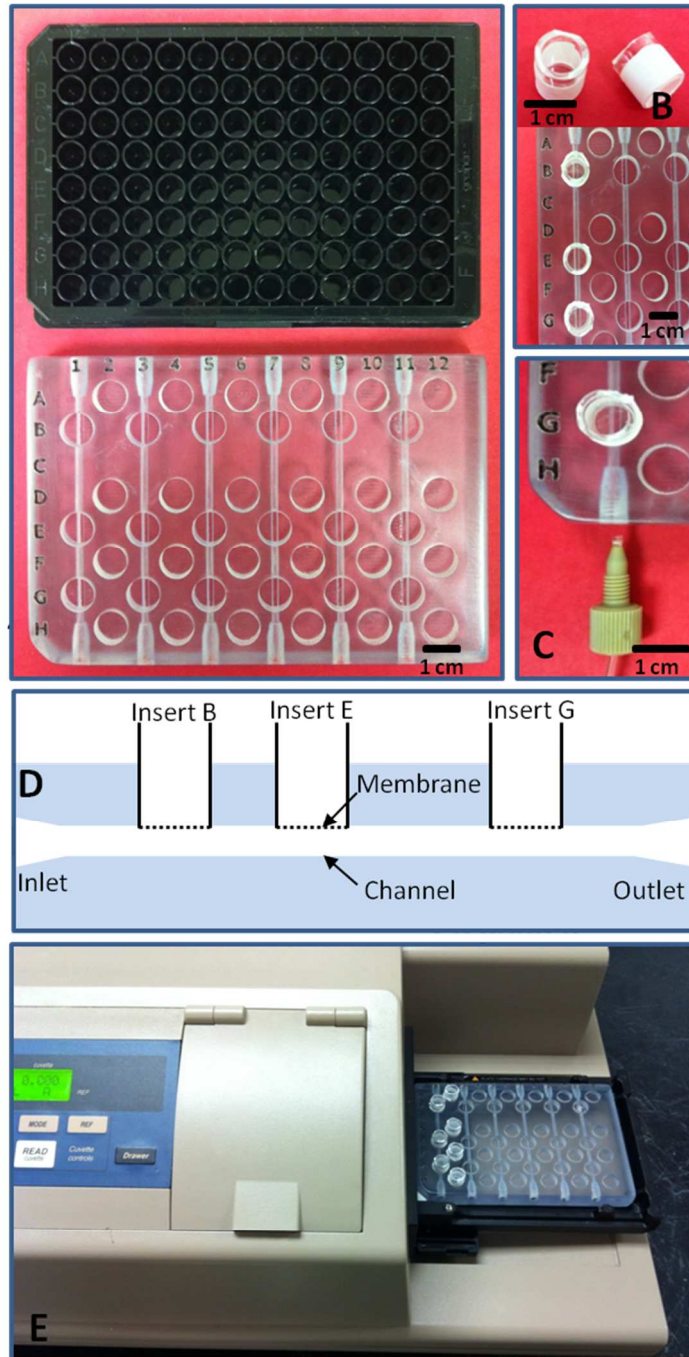
34
35
36 For those studies involving blood samples obtained from different donors, the standard error of
37 the mean was used in data evaluation. All other experiments utilized the standard deviation of
38 the mean for evaluation of precision. All statistical comparisons of obtained means were
39 performed using Student's t-test at 95% confidence, unless otherwise noted.
40
41
42
43
44
45

46 **Conclusion**

47
48 A 3-D printed fluidic device was successfully employed to facilitate the quantitative
49 determination of ATP release from ERYs stored in different conditions through the use of a plate
50 reader. In terms of preparing the materials necessary to evaluate the stored ERYs, 3-D printing
51 has proven to be a convenient method for device fabrication, is capable of printing devices that
52 can be used in conjunction with popular laboratory instrumentation (i.e., the device reported was
53
54
55
56
57
58
59
60

1
2
3 modeled after a 96-well plate, which is amenable to a commercial plate reader optical robotics
4 for efficient and high throughput analysis). Compared to conventional PDMS-based fluidic
5 devices, a 3-D printed device is more rugged and robust, did not leak between seals, and was
6 capable of multiple uses over a week-long study. Here, stored ERYs in AS-1 and AS-1N were
7 circulated and tested on a single 3-D printed device, thus significantly increasing the reliability of
8 the experimental data by eliminating variability of having to use multiple devices. The rigidity of
9 the material also creates an end-user friendly device. For example, threads can be directly
10 printed at the ends of each channel, allowing the channel to be connected to external tubing by
11 standard male leu adapters. Six channels integrated onto the device enable high throughput
12 flow analysis and static wells between channels facilitate simultaneous internal standard and/or
13 calibrators. Currently, the resolution 3-D printing technology and the required use of supporting
14 materials limit its application in producing single digit micro- or nanoscale-devices.
15 Furthermore, unlike soft-lithographic methods, where almost any laboratory can design and
16 fabricate fluidic devices, 3-D printers, especially high performance printers, are not widely
17 available. File transfer can help overcome some of the limitation of printer availability; however,
18 as new printers become available, this new method of fabricating fluidic devices is sure to have
19 an impact in the field.
20
21
22
23
24
25
26
27
28
29
30
31
32
33
34
35
36
37
38
39
40
41
42
43
44
45
46
47
48
49
50
51
52
53
54
55
56
57
58
59
60

FIGURE 1.



1
2
3
4
5
6
7
8
9
10
11
12
13
14
15
16
17
18
19
20
21
22
23
24
25
26
27
28
29
30
31
32
33
34
35
36
37
38
39
40
41
42
43
44
45
46
47
48
49
50
51
52
53
54
55
56
57
58
59
60

Figure 2.

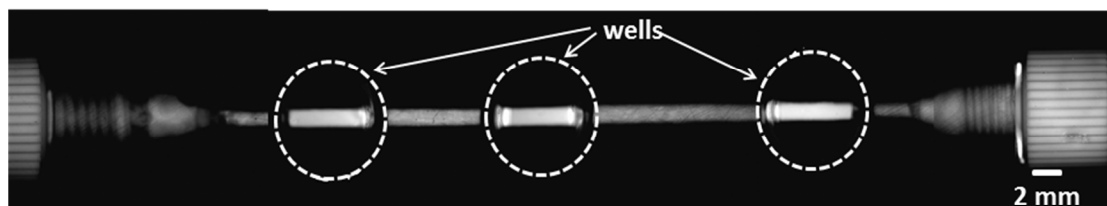
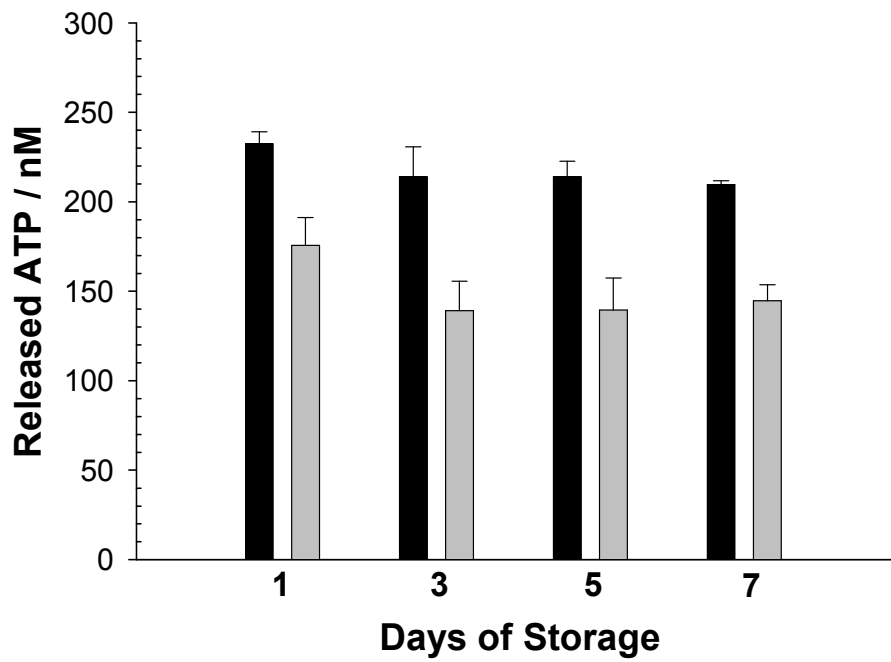


FIGURE 3.



1
2
3
4
5
6
7
8
9
10
11
12
13
14
15
16
17
18
19
20
21
22
23
24
25
26
27
28
29
30
31
32
33
34
35
36
37
38
39
40
41
42
43
44
45
46
47
48
49
50
51
52
53
54
55
56
57
58
59
60

Table 1. Remaining Volumes of Water in Inserts

Well	Remaining volume after 2 hour pumping/ μL^{a}	Well	Remaining volume after 2 hour loading/ μL^{b}
B1	49.5 ± 4.5	A2	48.7 ± 3.8
E1	48.6 ± 3.5	D2	49.4 ± 1.3
G1	46.8 ± 6.2	F2	47.6 ± 2.5

^a (n = 10; errors represent standard deviations)

^b (n= 3; errors represent standard deviations)

Table 2. Optimization of ATP Collection time^a

Collection time/min	Y intercept	Slope	R ²	Detection limit/nM
10	20.9 ± 5.5	517.5 ± 33.6	0.98 ± 0.00 ₅	136.6 ± 24.0
20	15.8 ± 1.8	565.4 ± 38.6	0.99 ± 0.00 ₁	52.4 ± 7.4
30	19.8 ± 1.0	883.8 ± 69.9	0.99 ± 0.00 ₇	33.3 ± 6.8

^a (n =3; all errors represent standard deviations)

Table 3. Optimization of Luciferin/luciferase Assay Volume^a

Assay volume/ μ L	Y intercept	Slope	R ²	Detection limit/nM
10	15.8 \pm 1.8	565.4 \pm 38.6	0.99 \pm 0.0 ₀₁	52.4 \pm 7.4
20	36.8 \pm 3.7	515.9 \pm 21.0	0.97 \pm 0.0 ₂	120.1 \pm 13.6
30	43.8 \pm 1.9	549.0 \pm 32.0	0.97 \pm 0.0 ₁	167.7 \pm 39.4

^a Each assay volume was performed on 5 ATP standards; the resultant calibration curves were evaluated for y-intercept, slope, and linearity which, in turn, were used to determine the detection limit. (n =3; all errors represent standard deviations)

Table 4. Observed quantitative detection of a 150 nM and 250 nM ATP standard from channel 1, channel 3, and channel 5^a

Known concentration/nM	150			250		
Observed concentration/nM	Ch1	Ch3	Ch5	Ch1	Ch3	Ch5
	140.6 ± 5.8	154.4 ± 7.2	159.4 ± 8.6	245.5 ± 15.6	253.7 ± 18.7	251.6 ± 14.0

^a Calibration curves were constructed from 5 ATP standards for each channel shown followed by determination of a sample with a known ATP concentration (150 or 250 nM). The recovered ATP is shown. (n =5; all errors represent standard deviations)

Table 5. Intra-channel Reproducibility Evaluation^a

	Y intercept	Slope	R ²	Detection limit/nM
Channel 1	15.8 ± 1.8	565.4 ± 38.6	0.99 ± 0.00 ₁	52.4 ± 7.3
Channel 3	18.7 ± 0.6	562.2 ± 12.1	0.99 ± 0.00 ₆	47.2 ± 7.4
Channel 5	15.3 ± 2.8	561.1 ± 18.3	0.98 ± 0.00 ₅	52.9 ± 5.2

^a (n =3; all errors represent standard deviations)

Figure Captions

Figure 1. A: The 3-D printed fluidic device (bottom) used in this study is modeled after the dimensions of a 96-well plate (top). Column and row markers make it convenient to localize wells. Six channels were printed on the odd number columns, with three wells corresponding to each channel. Static wells, printed on the even number columns allow for internal standards or calibration. B: Membrane inserts (top), which have a semi-permeable polyester membrane, are inserted into wells (bottom) of the 3-D printed device. C: Threads, printed at both ends of the channel, connect external tubing through a male leuc lock adaptor. D: A schematic cross section of a channel and the membrane inserts. E: The device locks into the sample holder of the commercial plate reader.

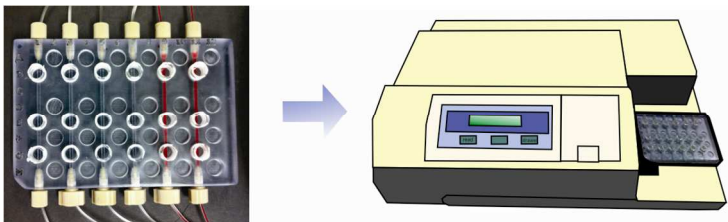
Figure 2. A fluorescence image of a channel after flowing fluorescein. The dotted circles indicate the well areas. The image implies that leakage of liquid from channel across the membranes did not occur. Due to the limited scope view, images on separate parts of the channel were obtained and integrated into a single image.

Figure 3. ATP released from ERYs stored in AS-1 (gray bars) and AS-1N (black bars). ATP was quantified with similar calibration curves as shown in Figure S3. There is a significant difference ($p < 0.03$; $p < 0.03$; $p < 0.01$ and $p < 0.03$ for Day 1, 3, 5 and 7, respectively) of released ATP from ERYs stored in two types of solutions for $n = 3$ humans. Error bars are standard error.

Reference

1. B. I. Whitaker, *2011 National Blood Collection and Utilization Survey*, American Association of Blood Banks, 2011.
2. J. E. Squires, *South. Med. J.*, 2011, **104**, 762-769.
3. B. D. Spiess, *Transfusion*, 2004, **44**, 4S-14S.
4. J. D. Roback, *Hematology Am. Soc. Hematol. Educ. Program*, 2011, **2011**, 475-479.
5. J. D. Roback, R. B. Neuman, A. Quyyumi and R. Sutliff, *Transfusion*, 2011, **51**, 859-866.
6. S. T. Halpin, K. B. Anderson, P. A. Vogel and D. M. Spence. *Open Nitric Oxide J.*, 2011, **3**, 8-15.
7. J. O. Lundberg, E. Weitzberg and M. T. Gladwin, *Nat. Rev. Drug Discov.*, 2008, **7**, 156-167.
8. S. Letourneau, L. Hernandez, A. N. Faris and D. M. Spence, *Anal. Bioanal. Chem.*, 2010, **397**, 3369-3375.
9. M. L. Ellsworth, C. G. Ellis, D. Goldman, A. H. Stephenson, H. H. Dietrich and R. S. Sprague, *Physiology (Bethesda)*, 2009, **24**, 107-116.
10. H. Zhu, R. Zennadi, B. X. Xu, J. P. Eu, J. A. Torok, M. J. Telen and T. J. McMahon, *Crit. Care Med.*, 2011, **39**, 2478-2486.
11. R. P. Patel, *Crit. Care Med.*, 2011, **39**, 2573-2574.
12. J. R. Hess, *J. Proteomics*, 2010, **73**, 368-373.
13. J. R. Hess, *Transfus. Apher. Sci.*, 2010, **43**, 51-59.
14. M. M. Engelgau, K. M. Narayan and W. H. Herman, *Diabetes Care*, 2000, **23**, 1563-1580.
15. C. D. Hillyer, *Blood banking and transfusion medicine: basic principles & practice*, Philadelphia, PA : Churchill Livingstone/Elsevier, 2007.
16. N. S. Mangalmurti, S. Chatterjee, G. J. Cheng, E. Andersen, A. Mohammed, D. L. Siegel, A. M. Schmidt, S. M. Albelda and J. S. Lee, *Transfusion*, 2010, **50**, 2353-2361.
17. Y. Wang, A. Giebink and D. M. Spence, *Integr. Biol.*, 2014, **50**, 65-75.
18. J. N. H. Shepherd, S. T. Parker, R. F. Shepherd, M. U. Gillette, J. A. Lewis and R. G. Nuzzo, *Adv. Funct. Mater.*, 2011, **21**, 47-54.
19. F. Ilievski, A. D. Mazzeo, R. E. Shepherd, X. Chen and G. M. Whitesides, *Angew. Chem. Int. Ed.*, 2011, **50**, 1890-1895.
20. K. B. Anderson, S. Y. Lockwood, R. S. Martin and D. M. Spence, *Anal. Chem.*, 2013, **85**, 5622-5626.
21. E. Sachs, M. Cima, P. Williams, D. Brancazio and J. Cornie, *J. Eng. Ind.-T. Asme*, 1992, **114**, 481-488.
22. F. P. W. Melchels, J. Feijen and D. W. Grijpma, *Biomaterials*, 2010, **31**, 6121-6130.
23. D. M. Karl and O. Holmhansen, *Anal. Biochem.*, 1976, **75**, 100-112.
24. A. W. Giebink, P. A. Vogel, W. Medawala and D. M. Spence, *Diabetes Metab. Res. Rev.*, 2013, **29**, 44-52.
25. C. X. F. Lam, X. M. Mo, S. H. Teoh and D. W. Hutmacher, *Mat. Sci. Eng. C-Bio. S.*, 2002, **20**, 49-56.
26. J. A. Meyer, J. M. Froelich, G. E. Reid, W. K. A. Karunaratne and D. M. Spence, *Diabetologia*, 2008, **51**, 175-182.
27. C. D. Hillyer, *Transfusion Medicine and Hemostasis: Clinical and Laboratory Aspects*, Philadelphia, PA : Churchill Livingstone/Elsevier, 2009.

1
2
3
4
5
6
7
8
9
10
11
12
13
14
15
16
17
18
19
20
21
22
23
24
25
26
27
28
29
30
31
32
33
34
35
36
37
38
39
40
41
42
43
44
45
46
47
48
49
50
51
52
53
54
55
56
57
58
59
60



A fluidic device constructed with a 3D-printer can be used to investigate stored blood components with subsequent high-throughput calibration and readout with a standard plate reader.